United Nations
Educational, Scientific and
Cultural Organization

ICTP - East African Institute
for Fundamental Research
under the auspices of UNESCO

Electron and hole mobilities of $Hg_5In_2Te_8$

Names: Elysée RUGWIRO

Reg N^o: 217192297

Supervised by: Dr. Omololu Akin-Ojo

ICTP-East African Institute for Fundamental Research (EAIFR)

University of Rwanda

June 18, 2024

The degree is awarded by the University of Rwanda

The degree is submitted in full fulfilment
The TURNITN anti-plagiarism check declaration

Declaration

I, Elysée RUGWIRO, with registration number 217192297, a student at the ICTP-East African Institute for Fundamental Research (EAIFR), University of Rwanda, College of Science and Technology (CST), hereby declare that this research study entitled " Electron and hole mobilities of Hg5In2Te8" under the supervisor of Dr. Omololu Akin-Ojo is my original work and has never been presented or submitted by someone else for any academic award in any university or institution of higher learning. Any contributions or ideas from others or my past work are properly acknowledged and referenced according to academic rules.

Student: Elysée Rugwiro

Supervisor: Dr. Omololu Akin-Ojo

Acknowledgement

I extend my appreciation to God for his love, grace, and strength that have been with me during my graduate studies. Also, I thank my supervisor Dr.Omololu Akin-Ojo for his critical guidance in my essay project, words and motivation can express my deep gratitude to him. I really appreciate his contribution of infinite price to my studies. I am deeply grateful to The World Academy of Sciences (TWAS) for their TWAS Grants, which provided me with a living allowance and covered my school fees. This crucial support made a significant impact on my life, and without it, I would not have been able to complete my studies. I sincerely appreciate TWAS for their substantial contribution to my academic journey. In general, I thank the whole team of Professors who taught us during this master's program. I also thank my family and my classmates who gave me all the support I needed. They sacrificed a lot to save the progress of my studies and shared life experiences particularly. In their kind heart, I got guidelines, motivation, and good advice that strengthened my studies. I would also like to express my gratitude to Ph.D. students Sosthène and Sunday for their valuable support and assistance. May the Almighty God bless all of them.

Abstract

High-mobility materials are important in modern-day electronic devices. This makes the search for materials with high mobilities of charge carriers unending. This study investigated $Hg_5In_2Te_8$ to examine the sizes of some of its parameters which contribute to the mobilities of charge carriers namely, the effective masses of holes and electrons in the system and its band gap. Computational parameters including kinetic energy cutoff, and the k mesh grid were first optimized to 40 Ry and $10 \times 10 \times 10$, respectively, in a series of preliminary DFT calculations. Using the DFT + U method, we then calculated the electronic band structure and density of states (DOS) of the material. The electronic band structure was obtained with an indirect energy gap of 0.0567 eV within the infrared range. Electron (m_e^*) and hole (m_h^*) effective masses were obtained by the finite difference method. The values obtained are ($m_{xx,e}^* = 0.024m_0$, $m_{yy,e}^* = 0.66m_0$, $m_{zz,e}^* = 0.012m_0$; $m_{xx,h}^* = 0.0034m_0$, $m_{yy,h}^* = 0.0034m_0$, $m_{zz,h}^* = 0.00547m_0$), indicating an enhanced charge carrier mobility. The density of states and conductivity effective masses, respectively, were determined to be $m_{e,Dos} = 0.057m_0$ and $m_{e,Cond} = 0.0238m_0$. Additionally, we calculated the electron and hole mobilities, where hole mobility is very high compared to the electron mobility ($\mu_{e,xx} = 14670\,\mathrm{cm}^2/(\mathrm{V.s})$, $\mu_{e,yy} = 533\,\mathrm{cm}^2/(\mathrm{V.s})$, $\mu_{e,zz} = 29340\,\mathrm{cm}^2/(\mathrm{V.s})$, $\mu_{h,xx} = 103555\,\mathrm{cm}^2/(\mathrm{V.s})$, $\mu_{h,yy} = 103555\,\mathrm{cm}^2/(\mathrm{V.s})$, $\mu_{h,zz} = 64367\,\mathrm{cm}^2/(\mathrm{V.s})$) when a typical electron collision time constant 0.2 ps was used. We conducted a comparative analysis with high-mobility materials like Silicon, Germanium, Gallium Arsenide, and mono-layer graphene to contextualize these findings. This investigation sheds light on the interesting electronic properties of $Hg_5In_2Te_8$. It provides valuable insights into its potential for advanced electronic and optoelectronic applications, particularly in high-performance semiconductors and infrared technology.

Contents

Abstract iii

1 Introduction 1
1.1 Background. 1
1.2 Electron mobility. 3
1.3 Holes mobility 4
1.4 Effective mass. 4
1.5 Problem statement. 6
1.6 Objectives. 6
1.6.1 Main objectives. 6
1.6.2 Specific objectives 6
1.7 Significance of the study. 6

2 Literature Review 8
2.1 Electronic, physical, and optical properties. 8
2.1.1 Electronic properties. 8
2.1.2 Topological insulator 10
2.1.3 Physical properties 11
2.1.4 Elastic constant 11

3 Methodology 12
3.1 Electronic structure calculation. 12
3.1.1 Schrödinger equation. 12
3.1.2 Kohn-Sham equations 12
3.1.3 Kohn-Sham total energy 13
3.1.4 SCF (Self-Consistent Field) calculation. 13
3.2 Effective mass calculation. 15
3.2.1 Formula. 15
3.2.2 Finite Difference Method. 15
3.3 Electrons and holes mobility calculation. 16

4 Results and Discussions 17
4.1 Best energy cutoff and k-point. 17
4.2 Cell parameters and atomic positions. 19
4.3 Electronic band structure. 20
4.4 Density of state (DOS). 22
4.5 Effective mass of $Hg_5In_2Te_8$. 25
4.5.1 Electron effective mass. 25
4.5.2 Hole effective mass. 25
4.6 Density of state effective mass. 26
4.7 Effective mass for conductivity. 27
4.8 Mobility 27
4.8.1 Electron mobility 27
4.8.2 Hole mobility 27

5 Conclusion and Recommendation. 28
5.1 Conclusion 28
5.2 Recommendation 28

References **30**

1 Introduction

1.1 Background.

Mobility is defined as the ability or capacity to move. In physics, mobility is related to the motion of charges (electrons, holes, and ions) under the influence of an applied external electric field. According to Drude's model[1][2], the mathematical expression for electron mobility μ is given by $\mu = e\tau/m^*$. This formula illustrates that mobility is directly proportional to the mean free time between collisions of the electron (τ) and inversely proportional to the effective mass (m^*) which means that the material with low effective mass should have a high mobility. Higher mobility implies that electrons can move more freely and efficiently through a material, experiencing fewer collisions. In practical terms, a material with high mobility is crucial for electronic devices as it enables faster charge transport, resulting in enhanced performance, reduced power consumption, and increased operational speed[3]. Therefore, the pursuit of high-mobility material is a key focus in the development of advanced semiconductor technologies, contributing to the optimization of electronic devices in various applications. $Hg_5In_2Te_8$ is a layered compound[4] composed of mercury (Hg), indium (In), and tellurium (Te) atoms. This type of compound with three elements is also known as a ternary compound. Ternary compounds have a wide range of properties and applications[5]. Currently, there is a high use of electronic and optical devices, like smartphones and computers. To make these devices work better and faster, scientists are on a mission to find the perfect materials to build them[6]. These researchers are looking for special materials that can make devices work better. They do this by studying the different properties of different materials such as electronic, optical, mechanical, physical, and chemical properties. Si, Ge, and GaAs are the most commonly used semiconductors for the application of (opto) electronic devices[7] due to their unique properties. $Hg_5In_2Te_8$ is a new semiconductor compound that has been proposed as a high mobility material for electronic devices. The unique crystal structure of $Hg_5In_2Te_8$ gives it high electron and hole mobility[8], which is a measure of how easily electrons and holes can move through a material. This high electron mobility makes it a promising candidate for use in a variety of electronic devices, including field-effect transistors, solar cells, and thermoelectric devices[9].

Specifically, Mobility is the ratio of the average drift velocity of charged particles and the magnitude of the electric field that is applied to the material. Mobility is an important property of semiconductors and other electronic materials, as it influences the speed and efficiency of charge transport through the material[10]. Higher mobility means that charged particles can move through the material more easily, resulting in faster electronic devices and more efficient energy conversion. Mathematically

$$\vec{v_{avg}} = \mu\vec{E} \tag{1.1}$$

Where v_{avg} is the average drift velocity of charge carriers, μ is electron (hole) mobility, and $\vec{E}$ is the applied electric field. This expression highlights that mobility is the ratio of the average drift velocity to the applied electric field strength.

In principles, the mobility of charged particles in a material is a 3×3 matrix. It is influenced by several factors, including the density and distribution of impurities or defects in the material, the temperature of the material, strength, and direction of the electric field applied to the material. Thus, it is an important parameter to consider when designing and evaluating electronic materials and devices. In some cases, the mobility of charged particles can be enhanced by adding dopants or other chemical modifiers to the material, which can alter the electronic properties of the material and improve charge transport. In semiconductor physics, there are two types of carriers: electrons and holes and each has its mobilities: μ_e (electron mobility) and μ_h (hole mobility), respectively. Electrons and holes are essential concepts in understanding the behavior of charge carriers in materials, particularly in semiconductors. Electrons carry negative charge and are responsible for electric current, while holes, conceptually representing positive charge carriers, can move in the opposite direction as electrons. Figure 1 shows the electron and hole in electronic configuration and Figure 2 shows the electrons in conduction band and holes in valence bands in semiconductor materials.

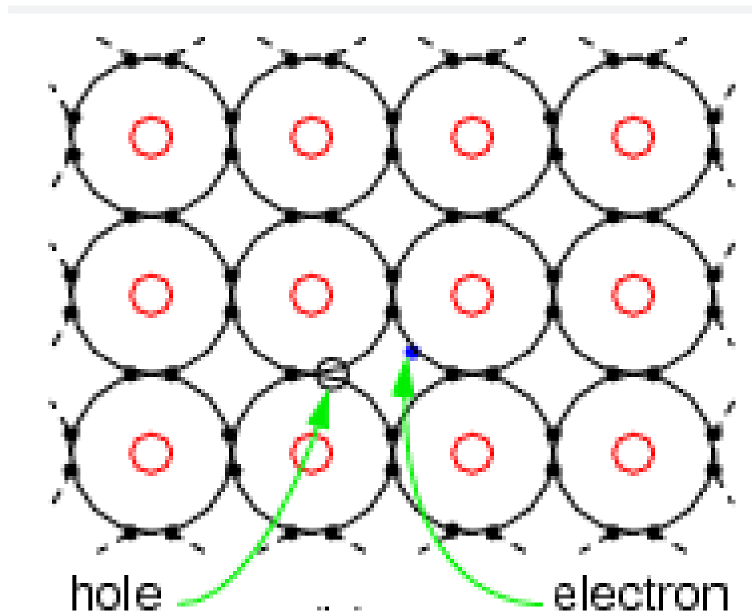

Figure 1: Electrons and Holes in the outermost shell.

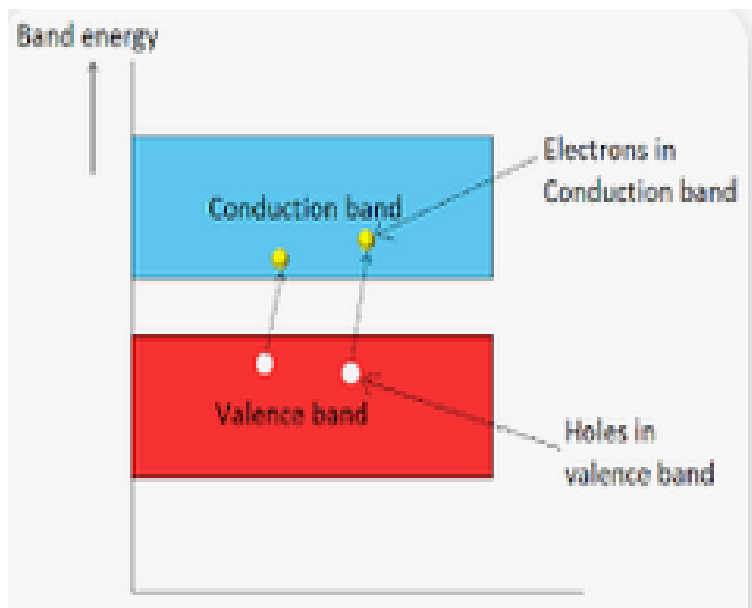

Figure 2: Electrons and Holes in conduction and valence band[11].

The mobility of the material is not enough to determine its potential in the application. An example of a material with high electron mobility but limited in different applications is graphene. Graphene is a two-dimensional material composed of carbon atoms arranged in a hexagonal lattice[12]. It has been found to have extremely high electron mobility, making it a promising material for high-speed electronic devices[13]. However, graphene has no band gap[14], which makes it difficult to turn off the flow of electrons in a device. This limits its usefulness in electronic devices such as transistors, which require the ability to turn on and off the flow of electrons.

The band structure and density of states of materials also play crucial roles in determining their electronic properties. $Hg_5In_2Te_8$ is a narrow-bandgap semiconductor, which means that it has a small energy gap between its valence and conduction bands [9]. The possible high mobility and narrow band gap of $Hg_5In_2Te_8$ make it a promising candidate for many applications. Other materials that have been reported to exhibit high electron mobility include gallium arsenide (GaAs) which is mostly used in the application of optoelectronic devices, Gadolinium Tellurium ($GdTe_3$). These materials have found applications in various electronic devices such as high-speed transistors, sensors, and photovoltaic cells.

In this work, we will discuss more about the effective mass of holes and electrons and how it is related to its potential application in electronic devices. We will do this by determining band structure and density of state by using Quantum Espresso. Quantum Espresso is an open-source, freely available software package for electronic structure calculations and materials modeling at the nanoscale [15]. It is based on density functional theory (DFT). DFT is a widely used method in condensed matter physics and chemistry for modeling the behavior of materials and molecules. Then we employ the finite difference method to calculate electron and hole effective mass.

1.2 Electron mobility.

Electron mobility refers to the ability of electrons to move through a material in response to an applied electric field. This is an important property in semiconductors and other electronic materials, where electrons are the primary charge carriers. In general, materials with high electron mobility have a high electrical conductivity and can be used to create high-speed electronic devices. $Hg_5In_2Te_8$ has been predicted to exhibit high electron mobility[4]. It is a fundamental property of materials and is related to the conductivity and transport properties of material. Electron mobility is very a important parameter in the study of electronic materials, as it determines the efficiency of charge transport and the ability of the material to conduct electricity. The high electron mobility of material tells the faster and more efficient charge transport, making material more suitable for electronic application. $GdTe_3$ is taken as the material with high electron mobility with electron mobility beyond $60,000 cm^2V^{-1}s^{-1}$ and effective mass of $m^* = 0.101$ to $0.106 m_0$ (m_0 is the free electron mass) [16]. In Table 1 below, there is another material with high electron and hole mobility [17][18][19][20].

Table 1: List of highest measured electron mobilities ($cm^2/(V.s)$)

Material	$\mu_e(cm^2/V.s)$	m_e^* (m_0)	$\mu_h(cm^2/V.s)$	m_h^* (m_0)
$GdTe_3$	60000	0.101	350	0.56
GaAs	8500	0.067	400	0.45
Graphene	20000	0.012	24000	0.016
GaN	1500	0.2	30	0.8
Ge	3900	0.041	1900	0.28
Si	1500	0.2	450	0.16

As listed in Table 1 there are many materials with high electron mobility such as graphene, GaAs, GaN, Ge, and Si semiconductors. Those materials are more interesting in research today because of their application. The research tells us that the $Hg_5In_2Te_8$ is also the compound with high mobility.

Graphene is the fastest electronic material known to date. The material with the highest electron mobility has more suitable applications but there are some limitations. The high electron of graphene is not enough to make it a suitable material for some applications. The low hole mobility makes it difficult to use as a p-type semiconductor

in conventional electronic devices. The band gap, production, cost, transport properties, and chemical stability can be the reason for not using graphene in different applications. Mobility plays a big role in material applications application, the material is used in any application depending on the band gap, structure of material, etc . . . .

1.3 Holes mobility

Hole mobility, on the other hand, refers to the ability of "holes" - or empty states in the valence band of a material to move through the material in response to an applied electric field. In some materials, such as p-type semiconductors, holes are the primary charge carriers. In these materials, a higher hole mobility leads to higher conductivity and faster electronic devices. The hole mobility of $Hg_5In_2Te_8$ is an important parameter for its use in thermoelectric and electronic applications. While the electron mobility of $Hg_5In_2Te_8$ is relatively high, there is limited research on its hole mobility. Some studies have reported that the hole mobility of $Hg_5In_2Te_8$ is lower than its electron mobility, but more research is needed to fully understand its hole transport properties.

1.4 Effective mass.

Effective mass is a concept used in solid-state physics to describe the behavior of electrons (or holes) in a crystal lattice. It is defined as the mass that a particle appears to have when it moves in response to an applied force, such as an electric field. The effective mass is a measure of how easily the particle can move through the crystal lattice, and it is related to the curvature of the energy bands that describe the motion of the particle in the crystal. Figure 3 shows the relationship between effective mass, mobility, and band curvature. It demonstrates that effective mass is inversely proportional to band curvature, meaning that a steeper curvature results in a lower effective mass. Conversely, mobility is directly proportional to band curvature, indicating that increased curvature leads to higher mobility.

The effective mass of an electron (or hole) can be either larger or smaller than the mass of a free electron (or hole) in a vacuum. In a semiconductor material, the effective mass of an electron (or hole) can vary depending on the direction of motion and the energy level of the particle. The effective mass is usually expressed as a ratio of the mass of the electron (or hole) in a vacuum to the effective mass, with the effective mass being greater than one for heavier electrons and less than one for lighter electrons.

The effective mass of electrons (or holes) is an important parameter in the design and optimization of semiconductor devices, as it affects the speed and efficiency of charge transport in the material. By controlling the effective mass of electrons (or holes), it is possible to tailor the electronic properties of the material and optimize its performance for a particular application.

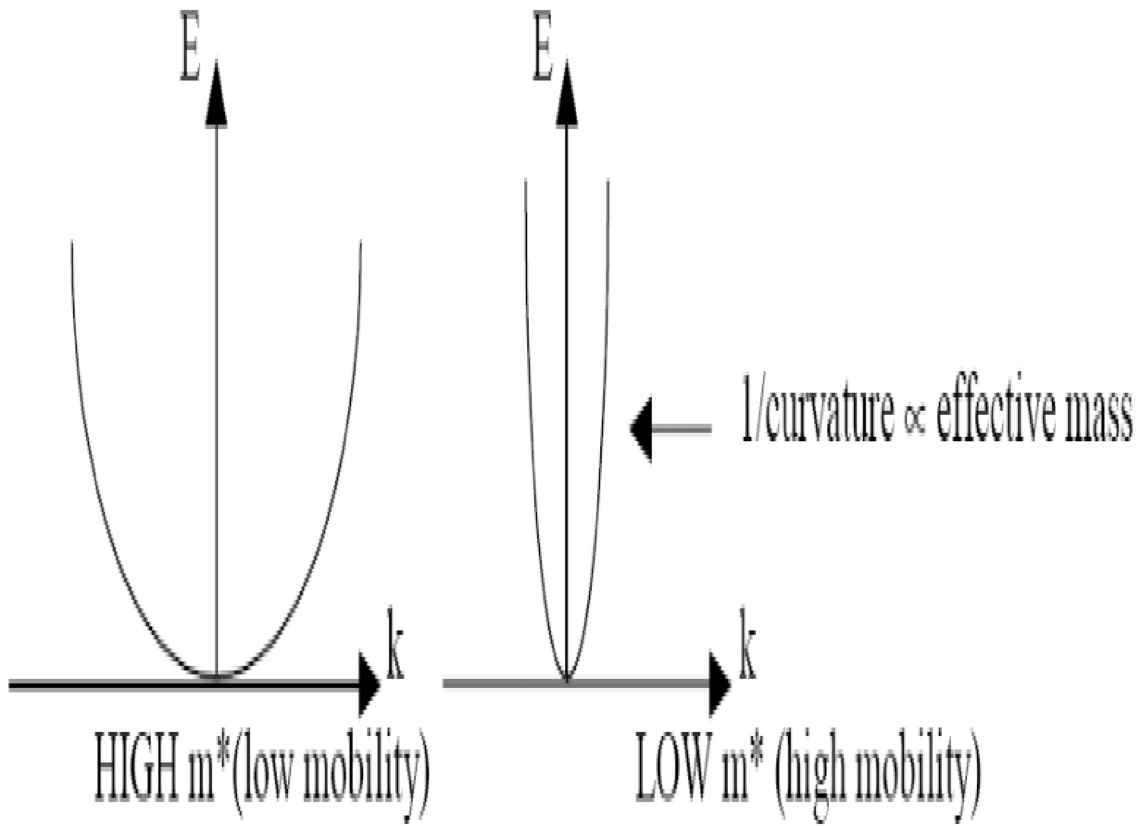

Figure 3: Relationship between effective mass, mobility, and band curvature[21].

1.5 Problem statement.

High-mobility materials are essential for the development of high-speed electronic devices, such as transistors. $Hg_5In_2Te_8$ is a narrow band-gap semiconductor with unique electronic properties that make it a promising candidate for use in electronic devices. However, the potential of $Hg_5In_2Te_8$ as a high mobility material is still unclear. This research aims to investigate the electronic properties of $Hg_5In_2Te_8$ to determine its potential as a high-mobility material. The results of this study will contribute to the understanding of the properties of $Hg_5In_2Te_8$ and its potential for use in high-speed electronic devices.

1.6 Objectives.

1.6.1 Main objectives.

The primary aim of this research is to determine the electron and hole mobilities of $Hg_5In_2Te_8$. This will contribute to an understanding of the electrical conductivity properties of this material and its potential applications in electronic devices.

1.6.2 Specific objectives

To achieve our main aim, we have the following specific objectives

- Determine the electronic band structure of $Hg_5In_2Te_8$
- Compute the density of states of $Hg_5In_2Te_8$
- Calculate the effective masses of holes and electrons in $Hg_5In_2Te_8$

1.7 Significance of the study.

The investigation of electronic band structures, the density of states, and effective mass is important in understanding electronic behavior and the potential of the material in different applications. This research is important for providing insight into the electronic properties of $Hg_5In_2Te_8$ as a new semiconductor material. This can determine the potential application of these new semiconductor materials in electronic devices, and more. The combination of DFT+U in Quantum Espresso software and the finite difference method provides a comprehensive computational framework for studying these properties and gaining deeper insights into the materials' electronic behavior.

The study in Ref [22] shows that $Hg_5In_2Te_8$ has a special shape and structure. It is made up of different kinds of ions like Hg_2^+ and Te_2^-. These atoms are arranged in a particular way in a space group called tetragonal $I-4m2$. The structure has two types of Hg_2^+ and Te_2^- sites. The Hg_2^+ atoms are connected to Te_2^- atoms to form tetrahedra (triangular pyramids). Some of these tetrahedra are also connected to In_3^+ atoms. The distances between the Hg and Te atoms vary depending on the site. The In_3^+ atoms are connected to Te_2^- atoms as well. The Te_2^- atoms have two different arrangements, with some bonded to Hg_2^+ and In_3^+ atoms in a specific pattern, and others forming another shape by bonding to Hg_2^+ and In_3^+ atoms. Overall, $Hg_5In_2Te_8$ has a complex structure with different atoms arranged uniquely. Figure 4 shows the conventional lattice of $Hg_5In_2Te_8$.

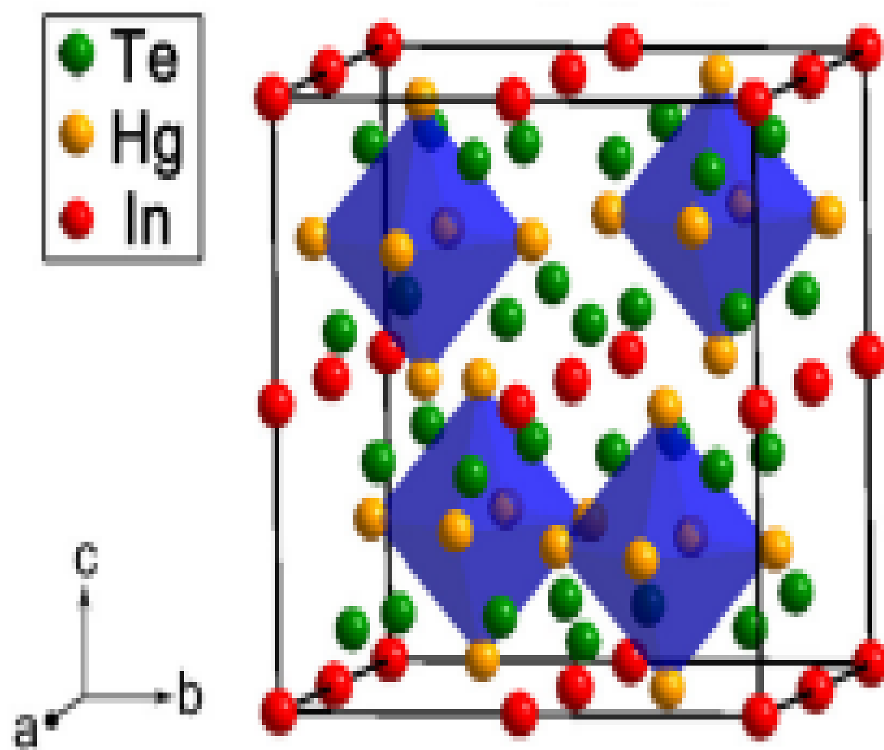

Figure 4: $Hg_5In_2Te_8$ conventional lattice [4].

2 Literature Review

In the 1970s researchers started synthesizing and studying $Hg_5In_2Te_8$ [23]. Its unique electronic and physical properties began to be recognized and studied in detail early in 2000. In 2003 researchers in Japan at the University of Tsukuba published a paper, in which they claimed that $Hg_5In_2Te_8$ exhibits a high electron mobility of over 20000 cm^2/Vs at low temperatures[24]. Previous studies have suggested that the material would have a low electron mobility due to its high carrier concentration. Because of this result, many researchers became interested and this led to further investigations into the material's electronic and physical properties. Although different properties were determined for the compound, the effective masses of its carriers have not been studied, as far as we know.

2.1 Electronic, physical, and optical properties.

The study in Ref [25] explores the crystal growth morphology and crystallography of $Hg_5In_2Te_8$ precipitates within an $Hg_3In_2Te_6$ matrix using transmission electron microscopy (TEM) and crystallographic models. It uncovers an unusual growth morphology of $Hg_5In_2Te_8$ with three crystallographically equivalent variants displaying different growth directions, suggesting a slight lattice constant variation during high-temperature phase transformation. The research emphasizes the significance of lattice mismatch-induced interface energy variation on precipitate growth and vacancy ordering phenomena in $Hg_5In_2Te_8$. These structural changes are pivotal as they greatly impact the electrical, mechanical, and optical properties of the material. $Hg_5In_2Te_8$ is known for its potential in various applications due to its unique properties, including excellent electrical conductivity, mechanical stability, and optical transparency, making it highly desirable for use in near-infrared photo-detectors and other semiconductor devices. Understanding the growth mechanism and crystallographic features influencing these properties is crucial for optimizing the performance of such applications and advancing semiconductor technology.

The Study in Ref [9] explores also the potential of $Hg_5In_2Te_8$ as a versatile material for high-efficiency photonic structures, owing to its unique properties as a defect semiconductor with a substantial concentration of stoichiometric vacancies. The study demonstrates its suitability for various photonic devices such as self-calibrating photodiodes, high-speed photodiodes, multi-element photodiodes with enhanced sensitivity, and optical filters covering a wide spectral range of $2 - 28\mu m$. Measurements reveal high sensitivity across a broad spectrum ($\lambda = 0.35 - 1.85\mu m$), comparable to established semiconductors like CdS, CdSe, GaAs, Si, and Ge. With its low melting point (983K), Hg3In2Te6 offers the potential for energy-efficient synthesis processes. Additionally, it exhibits high quantum efficiency in photoconductivity for photon energies from 0.74 to $3.5eV$ and is suitable for surface-barrier structures and hetero-junctions due to its low density of surface states and resistance to atmospheric oxygen absorption. These findings underscore the significant promise of $Hg_5In_2Te_8$ in advancing photonic technologies with improved performance, energy efficiency, and versatility.

The Study in Ref [4] explores the superstructures of the ternary compounds $HgIn_2Te_4$, $Hg_3In_2Te_6$, and $Hg_5In_2Te_8$, employing electron diffraction and conventional electron microscopy methods. Structural models are proposed, and an analysis of the domain structure, encompassing orientational and translational variants, is provided. Notably, the study focuses on the crystallography of $Hg_5In_2Te_8$, a compound of interest for its potential as a semiconductor in photovoltaic conversion and semiconductor superlattices. $Hg_5In_2Te_8$ is characterized by a metallic sublattice containing one vacant site every two face-centered cubic (fcc) subcells. Initial studies by Spencer identified an mm^2 symmetry for $Hg_5In_2Te_8$ and noted an order-disorder phase transition occurring at 445^0C. Subsequent work by Saunders and Seddon proposed a model for the ordered phase, comprising $2 \times 2 \times 2$ cubic zincblende-type subcells. This comprehensive analysis sheds light on the structural characteristics, defect behaviors, and phase transitions of these ternary compounds, providing insights into their suitability for advanced applications in electronic devices and optoelectronics. Special attention is given to the observation of periodic microtwins in $Hg_In_2Te_4$, contributing to a deeper understanding of their structural complexities.

2.1.1 Electronic properties.

$Hg_5In_2Te_8$ is a narrow band gap semiconductor with unique electronic properties that make it potentially suitable for various applications in electronic devices. From band structure, there are two types of energy gaps: direct and indirect band gap. A direct band gap is one in which the minimum energy level of the conduction band

(Conduction Band Minimum, CBM) and the maximum energy level of the valence band (Valence Band Maximum, VBM) occur at the same point in momentum space. The materials with direct band gaps are commonly used in optoelectronics, such as solar cells, LEDs (light-emitting diodes), and laser diodes, because they have high light emission and absorption efficiency. Which means that it can efficiently emit and absorb light. An indirect band gap is one in which CBM and VBM occur at a different point in momentum space. Figure 5 illustrates both direct and indirect band gaps. The study referenced in [26] on page 396 provides a precise determination of the energy gap of single-crystal $Hg_5In_2Te_8$ at a temperature of $300K$, yielding a value of $0.66eV$. This characterization is crucial for understanding the semiconductor properties of $Hg_5In_2Te_8$ and its potential applications in electronic devices, highlighting its suitability for various optoelectronic and photonic technologies.

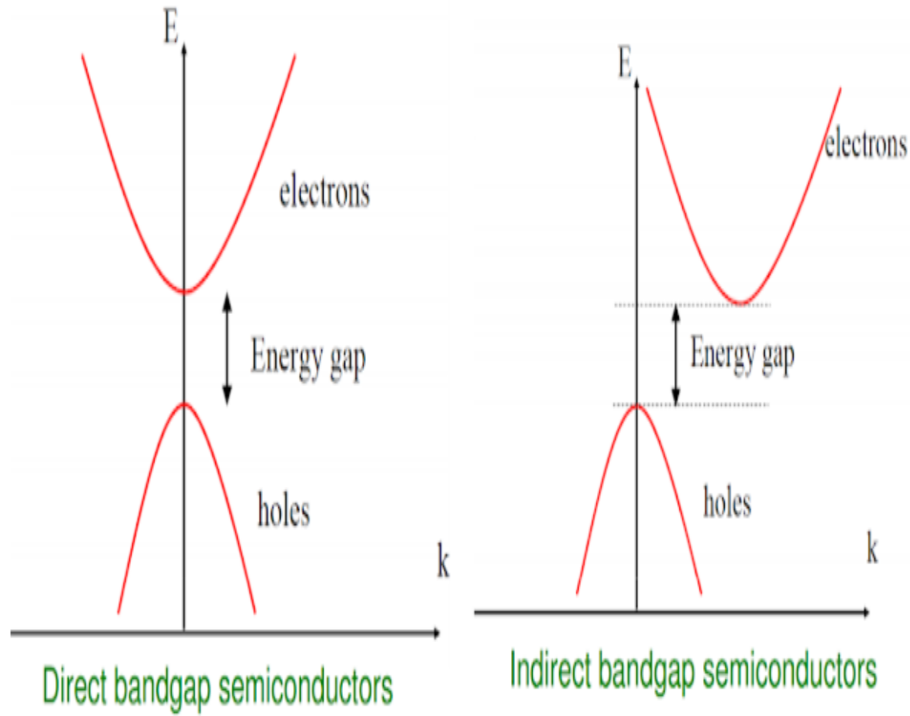

Figure 5: Direct and indirect band gap [27].

2.1.2 Topological insulator

$Hg_5In_2Te_8$ has also been proposed as a candidate for a topological insulator[28][29], a material that has a unique electronic structure that is insulating in the bulk but conductive on its surface [30]. Figure 6 illustrates the behavior of a topological insulator, highlighting the distinct properties of its interior and surface regions. This property makes $Hg_5In_2Te_8$ useful for potential applications in quantum computing and spintronics. Overall, the electronic properties of $Hg_5In_2Te_8$ make it a promising material for various electronic and optoelectronic applications, although more research is needed to fully understand and utilize its unique properties.

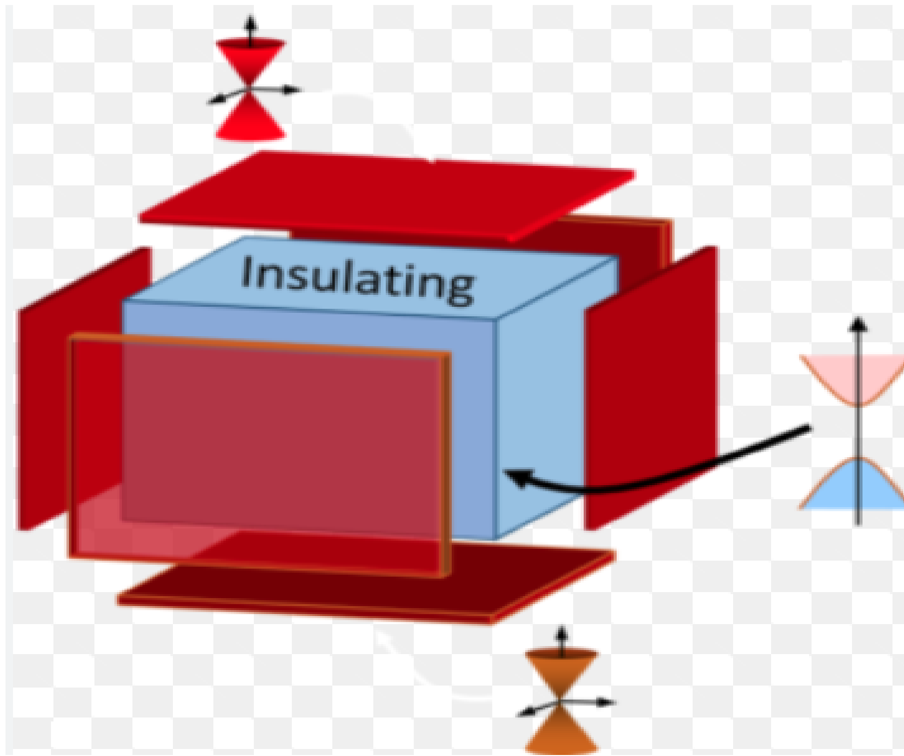

Figure 6: Topological insulator.

2.1.3 Physical properties

Hg5In2Te8 has a tetragonal crystal structure[4][25]. It is chemically stable at high temperatures and has a high melting point of around 709.3 degrees Celsius [31]. $Hg_5In_2Te_8$ is also a thermoelectric material, meaning that it can convert heat into electricity and vice versa. It has a relatively low thermal conductivity[31] and a high Seebeck coefficient[31], which are both important properties for efficient thermoelectric performance. $Hg_5In_2Te_8$ also exhibits a strong anisotropy in its physical properties, meaning that its properties can vary depending on the direction in which they are measured[32][33].

2.1.4 Elastic constant

The Study in Ref [34] investigates the elastic constants and crystal structure of the ternary compound semiconductor $Hg_5In_2Te_8$, filling a gap in the understanding of its mechanical properties. Through experimental methods including ultrasonic wave measurements and crystallographic analysis, the paper reveals crucial insights into the bonding nature, lattice dynamics, and mechanical response of $Hg_5In_2Te_8$. Comparisons with related II-VI compounds like HgTe and ZnS provide context for interpreting the results, highlighting similarities and differences in their elastic moduli and crystal structures. These findings not only deepen our understanding of $Hg_5In_2Te_8$ but also have implications for material design, device engineering, and theoretical modeling in the field of semiconductor materials science.

3 Methodology

The electronic properties of metals are reasonably explained by Drude's model. In 1900, Pauli Drude introduced an approach to elucidate the transport characteristics of electrons in metals. Essentially, with Ohm's law already firmly established, which delineates the relationship between current, voltage, and resistance of the material, Drude's model aimed to provide a comprehensive understanding of electron behavior in the context of electrical conduction. The mobility (μ) in the Drude model, defined as the ratio of the average drift velocity to the applied electric field, in terms of mean free time between collisions τ and effective mass m is expressed as $\mu = e\tau/m$. The electric conductivity (Σ) in terms of mobility and charge is given by $\Sigma = ne\mu$, where n is the number density of electrons.

For the calculation of electron and hole mobility in this work, we consider the following three steps to complete our task: In the first step we calculate the electronic band structure of $Hg_5In_2Te_8$, we did this by using the Quantum Espresso software. In the second step, we calculated the effective masses of electrons and holes of $Hg_5In_2Te_8$ from the band structure using the finite difference method. We completed our task by calculating electrons and hole mobility using effective masses obtained in the second step.

3.1 Electronic structure calculation.

In material science, electronic structure is the fundamental tool used to calculate a wide range of properties of material such as electronic, magnetic, and optical properties. By solving the many-electron Schrödinger equation, we calculate electronic structure represented by band structure and state density. We used local density approximation with the Hubbard U parameter to open the gap between the valence band and the conduction band.

3.1.1 Schrödinger equation.

Schrödinger's equation describes the many electron-nuclear systems. The Schrödinger equation is given by:

$$\hat{H}\psi(\mathbf{r}) = E\psi(\mathbf{r}) \tag{3.1}$$

where $\hat{H}$ is the many-particle electronic Hamiltonian operator that includes the kinetic energy, interaction between the electron and the external field (e.g field from ions) the electron-electron repulsion, and the on-site Coulomb interaction term with Hubbard parameter U, $\psi(\mathbf{r})$ is the wave function of the system and $\vec{r}$ represent the positions of all N electrons in the system. In mathematical notation, the Hamiltonian operator can be written as:

$$\hat{H} = -\frac{\hbar^2}{2m}\sum_{i=1}^{N}\nabla_i^2 + \sum_{i=1}^{N} v(\mathbf{r}_i) + \frac{1}{2}\sum_{i\neq j}^{N}\frac{1}{|\mathbf{r}_i - \mathbf{r}_j|} + U\sum_{i=1}^{N} n_{i\uparrow}n_{i\downarrow} \tag{3.2}$$

Where N is the total number of particles, ∇_i^2 is the Laplacian operator acting on the i_{th} particle, $v(\mathbf{r}_i)$ is the external potential acting on the i_{th} particle, $|\mathbf{r}_i - \mathbf{r}_j|$ is the distance between the i_{th} and j_{th} particles, $ni\uparrow$ and $ni\downarrow$ are the spin-resolved occupation numbers of the i_{th} particle, and U is the Hubbard parameter. The third term of equation 3.2 is an addition term to the standard Density Functional Theory (DFT) method. This term represents the on-site coulomb interaction between electrons with opposite spins at the same spatial location. It was introduced in DFT calculation to better capture the effects of on-site Coulomb interactions, especially in materials where the standard DFT methods may not provide accurate descriptions of electronic correlation. The wave function $\psi(\mathbf{r})$ satisfies the Schrödinger equation and contains all the information about the system. The goal of solving the Schrödinger equation is to obtain the wave function and the corresponding energy eigenvalue E.

3.1.2 Kohn-Sham equations

It is complicated to solve the Schrödinger equation of many electrons' systems. With local density approximation in DFT, we approximate equation 3.2 of the Kohn-Sham equation to calculate the electron structure of $Hg_5In_2Te_8$. The Kohn-Sham equation is the one-electron Schrödinger equation of non-interacting electrons that generate the same electron density. The Kohn-Sham equation is given by the following equation:

$$\left[-\frac{1}{2}\nabla^2 + v_{\text{eff}}(\mathbf{r})\right]\psi_i(\mathbf{r}) = \varepsilon_i\psi_i(\mathbf{r}) \tag{3.3}$$

In equation 3.3, $\psi_i(\mathbf{r})$ is the i_{th} single-particle wave function, ε_i is the corresponding eigenvalue, $v_{\text{eff}}(\mathbf{r})$ is the effective potential that includes the exchange-correlation potential and the on-site Coulomb interaction term, U is the Hubbard U parameter, and $n_{i\uparrow}(\mathbf{r})$ and $n_{i\downarrow}(\mathbf{r})$ are the spin-resolved occupation numbers of the correlated orbital at position $\mathbf{r}$.
We used $\hbar = m = 1$.

$$v_{eff} = V_{ext} + V_H[n(r)] + V_{xc}(r) + U\sum_i n_{i\uparrow}n_{i\downarrow} \tag{3.4}$$

Equation 3.4 is Kohn-Sham's potential energy, Where:
V_{ext} external potential: is the potential energy of electron-nuclei interaction, $V_H[n(r)]$ Hartree potential: is the electrostatic potential from electron charge density. It calculated from:$\nabla^2 V_H[n(r)] = -4\pi n(r)$ where n(r) $=-e\sum_i |\Psi|^2$ and

$V_{xc}(r)$ exchange-correlation potential: is an electron-electron interaction potential.

3.1.3 Kohn-Sham total energy

The Kohn-Sham total energy is the ground state energy in the function of electron density. The Kohn-sham total energy is given by:

$$E_{\text{KS}}[\rho] = \sum_{i=1}^{N_{\text{occ}}} \langle\psi_i|\hat{T}|\psi_i\rangle + \int V_{\text{ext}}(\mathbf{r})\rho(\mathbf{r})d\mathbf{r} + E_{\text{Hxc}}[\rho] + E_U[\rho] \tag{3.5}$$

where $E_{\text{KS}}[\rho]$ is the Kohn-Sham energy functional, N_{occ} is the number of occupied Kohn-Sham orbitals, $\langle\psi_i|\hat{T}|\psi_i\rangle$ is the kinetic energy of the $i-th$ orbital, $V_{\text{ext}}(\mathbf{r})$ is the external potential acting on the system, $\rho(\mathbf{r})$ is the electron density, $E_{\text{Hxc}}[\rho]$ is the exchange-correlation energy functional, and $E_U[\rho]$ is the on-site Coulomb interaction energy functional with Hubbard U parameter.
The on-site Coulomb interaction energy functional can be expressed as:

$$E_U[\rho] = \frac{1}{2}U\sum_{\sigma=\uparrow,\downarrow}\int n_\sigma(\mathbf{r})n_{\bar{\sigma}}(\mathbf{r})d\mathbf{r} \tag{3.6}$$

where U is the Hubbard U parameter, $n_\sigma(\mathbf{r})$ is the spin-resolved electron density, and $\bar{\sigma}$ denotes the opposite spin state. This term takes into account the additional energy cost associated with the double occupancy of a localized orbital, which is the essence of the LDA+U and GGA+U methods.

3.1.4 SCF (Self-Consistent Field) calculation.

To run electronic structure calculation, we used pw.x. We did this by solving the Kohn-Sham equation by creating a self-consistency quantum espresso input file ($Hg_5In_2Te_8$.scf.in). Scf calculation tests the convergence of the input file and by self-consistent calculation, we determine the ground-state electron density, total energy, valence, and conduction band energy of the system. Figure 7 presents the self-consistent field (SCF) calculation flowchart. It outlines the steps in the SCF process, starting from the initial input and progressing through each stage to the final output. The output($Hg_5In_2Te_8$.scf.out) contains electronic structure information, such as the band structure and density of states.
The initial input file was obtained from the Material Project database available at https://next-gen.materialsproject.org/materials/mp-1212052. Once acquired, we conducted a series of optimization procedures to refine the accuracy of our self-consistent calculations. This involved performing relaxation ($relax$) and variable-cell relaxation ($vc-relax$) calculations to achieve the most stable and energetically favorable atomic arrangement. To enhance the precision of our calculations, we systematically determined the optimal parameters for energy cutoff ($ecut$) and the sampling of the Brillouin zone using k_{-} points. through these iterative steps, we aimed to attain a refined and reliable representation of the material's electronic structure and properties.

The Hubbard U parameters applied in our study are 8.98 eV for Indium (In), 0.73 eV for Tellurium (Te), and 0.55 eV for Mercury (Hg), aimed at accurately accounting for on-site Coulomb interactions in our electronic structure calculations. For In, the value of 8.98 eV is sourced from [35], addressing the correlation effects of the In-4d orbitals. For Te, the 0.73 eV value, applied to the Te-5p orbitals, is from [36], and for Hg, the 0.55 eV value for the Hg-5d orbitals is from the Materials Project database https://contribs.materialsproject.org/projects/hubbard. These values, chosen based on their proven effectiveness in similar systems, are not universally transferable but were validated specifically for our system through convergence tests. We employed ortho-atomic projectors for the Hubbard U correction because they generally provide more accurate results, such as atomic occupations, compared to atomic projectors, due to their ability to better represent the local environment. By integrating these parameters, we aimed to enhance the reliability and precision of our electronic structure calculations, particularly considering the filled d-orbitals of these elements.

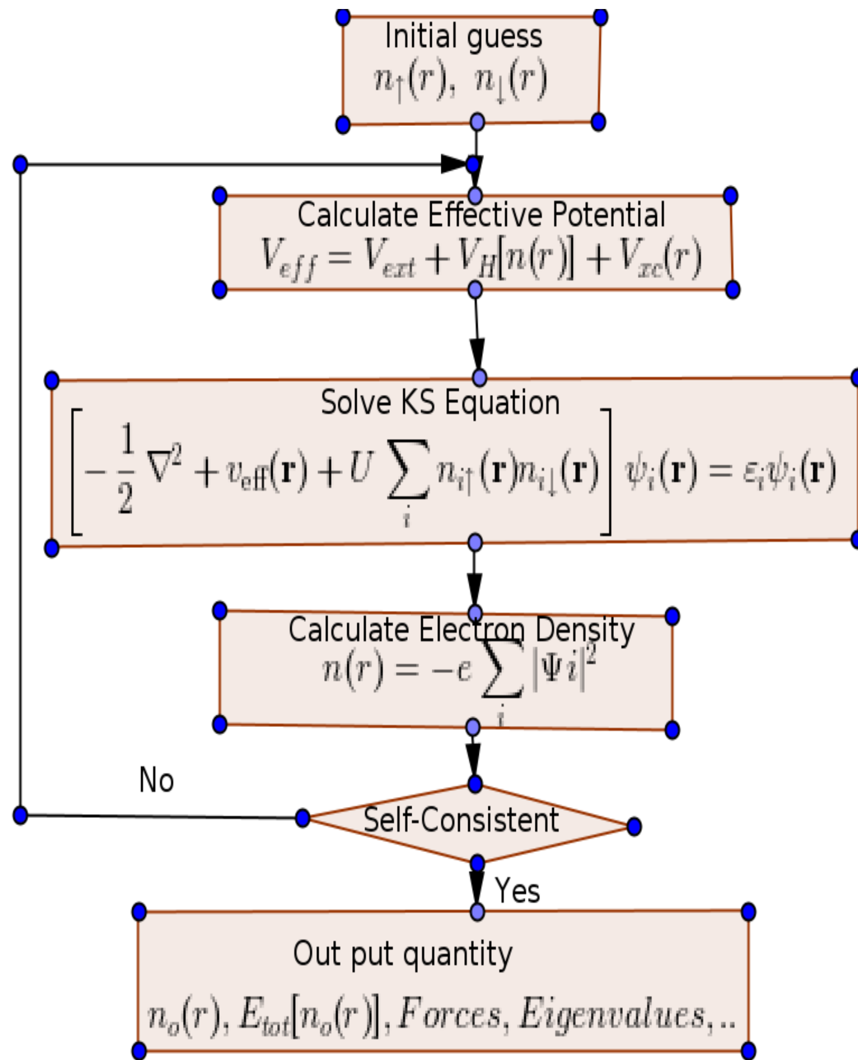

Figure 7: scf calculation flowchart

3.2 Effective mass calculation.

This is the second step in our job. Effective masses are parameters that describe the curvature of the energy bands near the band extreme. It is a symmetric matrix tensor where the diagonal elements represent the curvature of band dispersion in the direction of the Cartesian axes and off-diagonal elements represent the coupling between different directions. Effective mass determines how easily charge carriers can move through the material in response to an applied electric field. In this project, we used *bands.x* code in Quantum ESPRESSO to calculate the effective mass of $Hg_5In_2Te_8$.

3.2.1 Formula.

$$\frac{1}{m_{ij}^*} = \frac{1}{\hbar^2}\left(\frac{\partial^2 E(\mathbf{k})}{\partial k_i \partial k_j}\right)_{\mathbf{k}=\mathbf{k_0}} \tag{3.7}$$

Where:

- $E(\mathbf{k})$ is the electronic energy as a function of wave-vector,
- $\mathbf{k}$=$\mathbf{k_0}$ is the wave-vector at which band extremum occurs,
- m_{ij}^* is the effective mass tensor,
- $\hbar$ is the reduced Planck constant.

The second derivative of the energy to the wave vector is a matrix of partial derivatives with elements given by:

$$\frac{\partial^2 E(\mathbf{k})}{\partial k_i \partial k_j} = \frac{\hbar^2}{m_{ij}^*} \tag{3.8}$$

Where i and j represent the Cartesian coordinates of the wave vector $\mathbf{k}$.

3.2.2 Finite Difference Method.

Take the second derivative of the wave function to the position in the x, y, and z directions using the finite difference method. The finite difference method involves approximating the second derivative using a small step size in each direction. For example, the second derivative in the x-direction can be approximated as:

$$\frac{\partial^2 E}{\partial k_x^2} \approx \frac{E(k_x + \Delta k_x) - 2E(k_x) + E(k_x - \Delta k_x)}{(\Delta k_x)^2} \tag{3.9}$$

where E is the energy, Δk_x is the step size, and x is the position in the x-direction. Calculate the effective mass in each direction (x, y, and z) using the curvature of the wave function and the energy eigenvalues. The electron and hole effective mass is given by:

$$m_{c,v}^* = \hbar^2/(\partial^2 E/\partial k^2) \tag{3.10}$$

where $m_{c,v}^*$ is the effective mass of the conduction or valence band, $\hbar$ is the reduced Planck constant, E is the energy eigenvalue, and k is the wave vector.
In general, the first derivative is:

$$\frac{\partial E}{\partial k_i} \approx \frac{E(k_1, ..., k_i + \Delta k_i, ..., k_n) - E(k_1, ..., k_i - \Delta k_i, ..., k_n)}{2\Delta k_i} \tag{3.11}$$

where E is the band energy, k_i is the wave vector along the i_{th} direction, n is the number of directions in reciprocal space, and Δk_i is the spacing between neighboring k-points along the i_{th} direction.

Calculate the curvature of the energy bands using the second derivative of the energy with respect to k:

$$\frac{\partial^2 E}{\partial k_i^2} \approx \frac{E(k_1, ..., k_i + \Delta k_i, ..., k_n) - 2E(k_1, ..., k_i, ..., k_n) + E(k_1, ..., k_i - \Delta k_i, ..., k_n)}{\Delta k_i^2} \tag{3.12}$$

$$\frac{\partial^2 E}{\partial k_i \partial k_j} \approx \frac{E(k_i + \Delta k_i, k_j + \Delta k_j) + E(k_i - \Delta k_i, k_j - \Delta k_j) - E(k_i - \Delta k_i, k_j + \Delta k_j) - E(k_i + \Delta k_i, k_j - \Delta k_j)}{4\Delta k_i \Delta k_j} \tag{3.13}$$

Calculate the effective mass tensor components using the curvature of the energy bands:

$$m_{ij}^* = \frac{\hbar^2}{\frac{\partial^2 E}{\partial k_i \partial k_j}} \tag{3.14}$$

where m_{ij}^* is the i, j_{th} component of the effective mass tensor, and $\hbar$ is the reduced Planck constant. Diagonalize the effective mass tensor to obtain the principal axes and the corresponding effective masses.
This procedure provides an estimate of the effective mass tensor components for a given crystal structure and a k-point path in reciprocal space. The accuracy of the results depends on the density of the k-point mesh, the choice of the Brillouin zone sampling, and the level of theory used to solve the Kohn-Sham equation.

3.3 Electrons and holes mobility calculation.

We complete our task by calculating electron mobility. The mobility is inversely proportional to the effective masses. With effective mass calculated in step 2, we were able to calculate electrons and hole mobility.
The electron mobility can be calculated in terms of the effective mass using the following equation:

$$\mu = \frac{e\tau}{m^*} \tag{3.15}$$

where μ is the electron mobility, e is the elementary charge, τ is the relaxation time, and m^* is the effective mass of the electron.

4 Results and Discussions

This chapter includes the figures and tables of results obtained in the different calculations in our study.

4.1 Best energy cutoff and k-point.

The optimal energy cutoff that effectively refines our results was determined to be $40Ry$. This selection was made through a systematic analysis where we plotted the relationship between energy and energy cutoff, as illustrated in Figure 8. Similarly, for the ideal k-point parameter, we identified that 10 offered the most favorable convergence. This conclusion was drawn from the energy versus k-point plot as shown in Figure 9. The pseudopotential used in this calculation for the three elements are Hg.pbe-n-kjpaw_psl.1.0.0.UPF for Mercury, In.pbe-n-kjpaw_psl.1.0.0.UPF for Indium, and Te.pbe-n-kjpaw_psl.1.0.0.UPF for Tellurium. Also, local density function theory (LDA+U) was used to optimize the result.

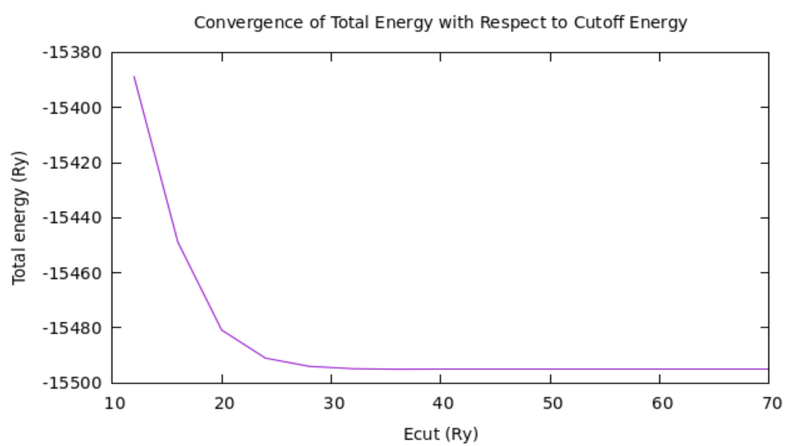

Figure 8: Total energy vs E_cut

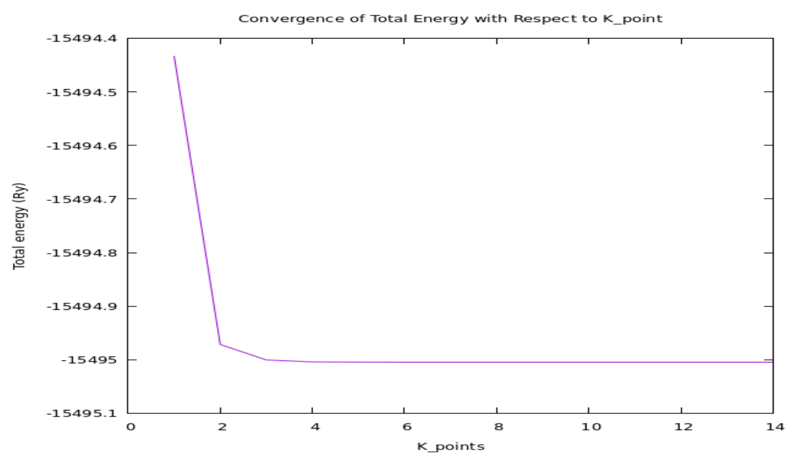

Figure 9: Total energy vs k_points

4.2 Cell parameters and atomic positions.

After getting the best energy cutoff and k-point we also find the best cell parameter and atomic position for the 30 atoms unit cell of $Hg_5In_2Te_8$. Table 2 presents the computed lattice parameters, which are slightly larger than the ones from the material project database (a = 9.16, b = 9.16, c = 12.78) Angstroms. The atomic positions used in our calculations are detailed in Table 3. These results were obtained through a two-step process: the vc-relax calculation was used to optimize the cell parameters, and the relax calculation was performed to optimize the atomic positions. Our findings indicate that $Hg_5In_2Te_8$ crystallizes in a tetragonal structure with the space group I42. This conclusion is supported by the lattice parameters and the atomic positions listed in the tables.

x	y	z
9.252629139	0.000000000	0.000000000
0.000000000	9.252629139	0.000000000
0.000000000	0.000000000	12.925102764

Table 2: CELL_PARAMETERS (angstrom)

Atom	x-coordinate	y-coordinate	z-coordinate
In	0.0000000000	0.0000000000	0.2465424580
In	0.0000000000	0.0000000000	0.7534575420
In	0.5000000000	0.5000000000	0.7465411613
In	0.5000000000	0.5000000000	0.2534588387
Hg	0.5000000000	0.0000000000	0.2500011868
Hg	0.2723335362	0.7276664638	0.5000000000
Hg	0.7276664638	0.2723335362	0.5000000000
Hg	0.2276660624	0.2276660624	0.0000000000
Hg	0.2723335362	0.2723335362	0.5000000000
Hg	0.0000000000	0.5000000000	0.7499988132
Hg	0.7723339376	0.2276660624	0.0000000000
Hg	0.2276660624	0.7723339376	0.0000000000
Hg	0.7276664638	0.7276664638	0.5000000000
Hg	0.7723339376	0.7723339376	0.0000000000
Te	0.0000000000	0.2703932647	0.1418263611
Te	0.0000000000	0.7296067353	0.1418263611
Te	0.7703937762	0.5000000000	0.3581736514
Te	0.2296062238	0.5000000000	0.3581736514
Te	0.0000000000	0.2489628339	0.6194191294
Te	0.5000000000	0.2510372100	0.1194193616
Te	0.2489628339	0.0000000000	0.3805808706
Te	0.2510372100	0.5000000000	0.8805806384
Te	0.5000000000	0.7703937762	0.6418263486
Te	0.5000000000	0.2296062238	0.6418263486
Te	0.2703932647	0.0000000000	0.8581736389
Te	0.7296067353	0.0000000000	0.8581736389
Te	0.5000000000	0.7489627900	0.1194193616
Te	0.0000000000	0.7510371661	0.6194191294
Te	0.7489627900	0.5000000000	0.8805806384
Te	0.7510371661	0.0000000000	0.3805808706

Table 3: Atomic positions in the crystal structure of $Hg_5In_2Te_8$.

4.3 Electronic band structure.

Through a self-consistent calculation, we have determined the highest occupied energy level, denoted as $E_v = 4.7934eV$ at wave-vector $k_{max} = (0, 0.125, 0)$, and the lowest unoccupied energy level, represented as $E_c = 4.8501eV$ at wave-vector $k_{min} = (0, 0, 0)$. Notably, the band structure of $Hg_5In_2Te_8$ is illustrated in Figure 10, revealing an indirect energy gap, $E_g = 0.0567eV$, situated within the infrared range. This particular energy gap opens the door to several applications in infrared technology, encompassing infrared sensing and imaging, advanced communication systems, efficient photovoltaic materials, medical diagnostics, and more. From material project database the energy gap of $Hg_5In_2Te_8$ is $E_g 0.01eV$ which is significantly smaller than $E_g = 0.0567eV$ calculated in this study. The difference between our calculated band gap and the value from the Material Project database is due to the inclusion of the Hubbard U parameter in our calculations, which effectively opens the energy gap. Despite this small difference, both values indicate a small indirect band gap.

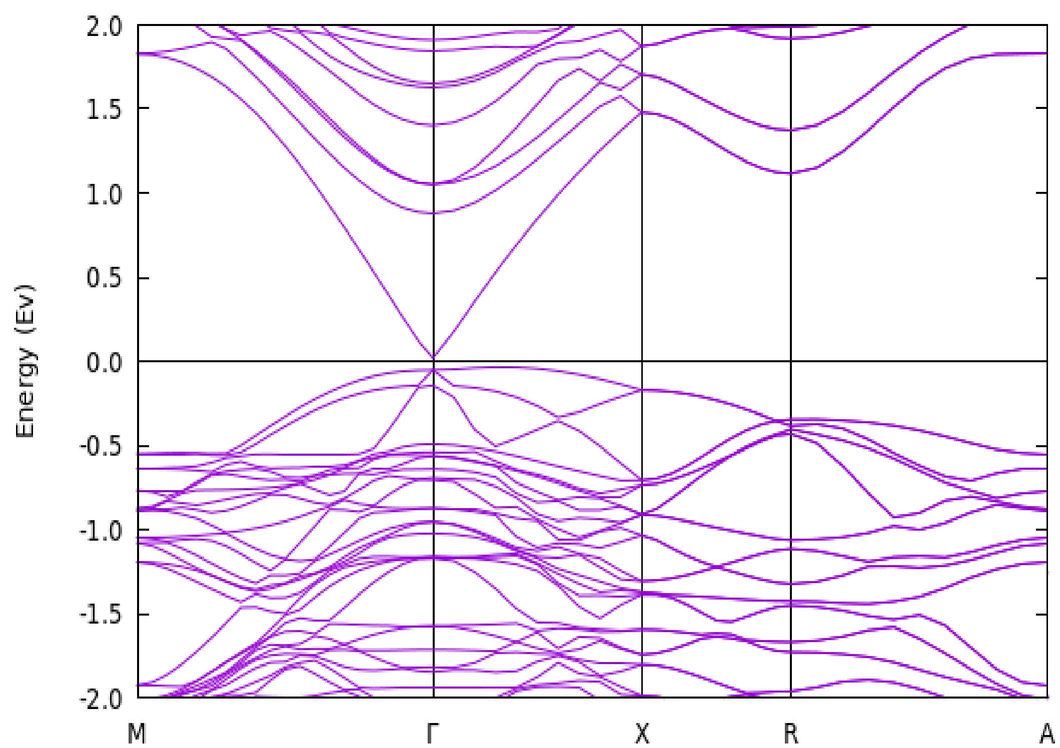

Figure 10: $Hg_5In_2Te_8$ band structure.

4.4 Density of state (DOS).

Figure 11 shows the density of state curve. It describes the distribution of energy states for particles, such as electrons in a solid, within a given range. In other words, the density of states tells us how many energy states there are per unit energy interval. The information provided by the density of state tells us about the state available in ΔE in both conduction and valence bands. The more state in the conduction band means that the material can conduct electricity easily. Figure 12 shows The projected density of state (PDOS) curve. The PDOS helps in understanding the detailed electronic structure by breaking down the total DOS into contributions from specific atomic orbitals and atoms. The large peaks of p orbitals of Hg, In, and Te in both the valence and conduction band means that the electronic structure of the $Hg_5In_2Te_8$ is mainly influenced by the p orbitals of these elements. In the valence band, Te p orbitals are the most significant, indicating strong bonding interactions. In the conduction band, Hg p orbitals dominate, highlighting their crucial role in the material's conductive properties. This means that when electrons get excited from the valence band to the conduction band, they primarily move between these p orbitals. This efficient electron movement improves the material's electrical and optical properties.

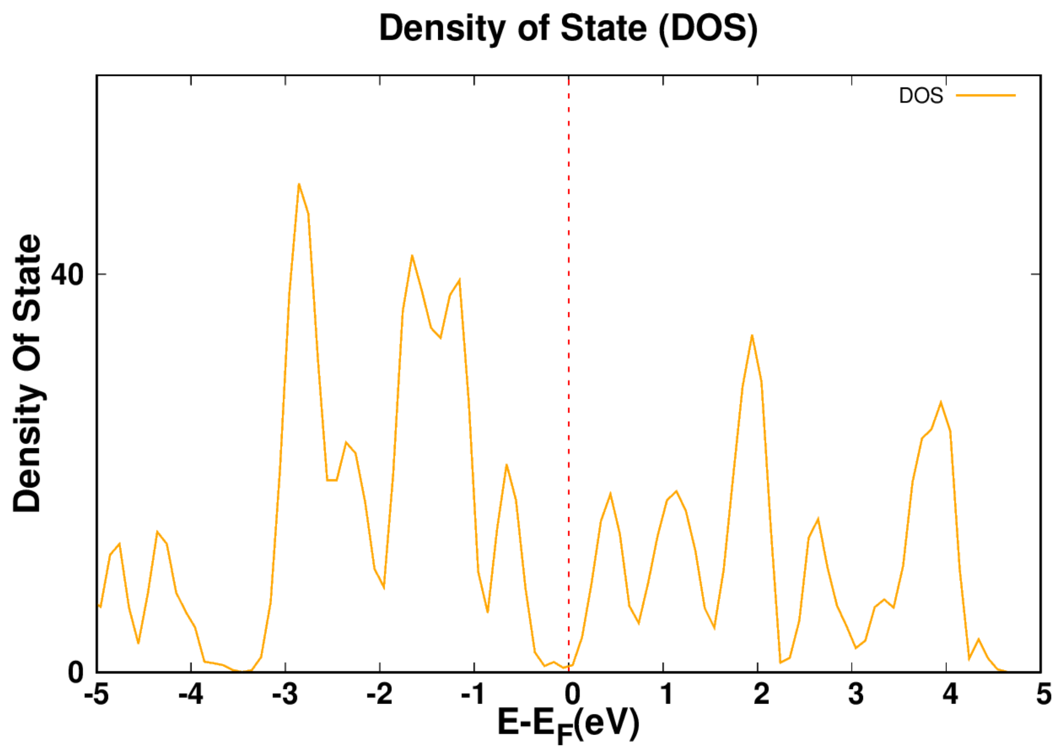

Figure 11: $Hg_5In_2Te_8$ density of state.

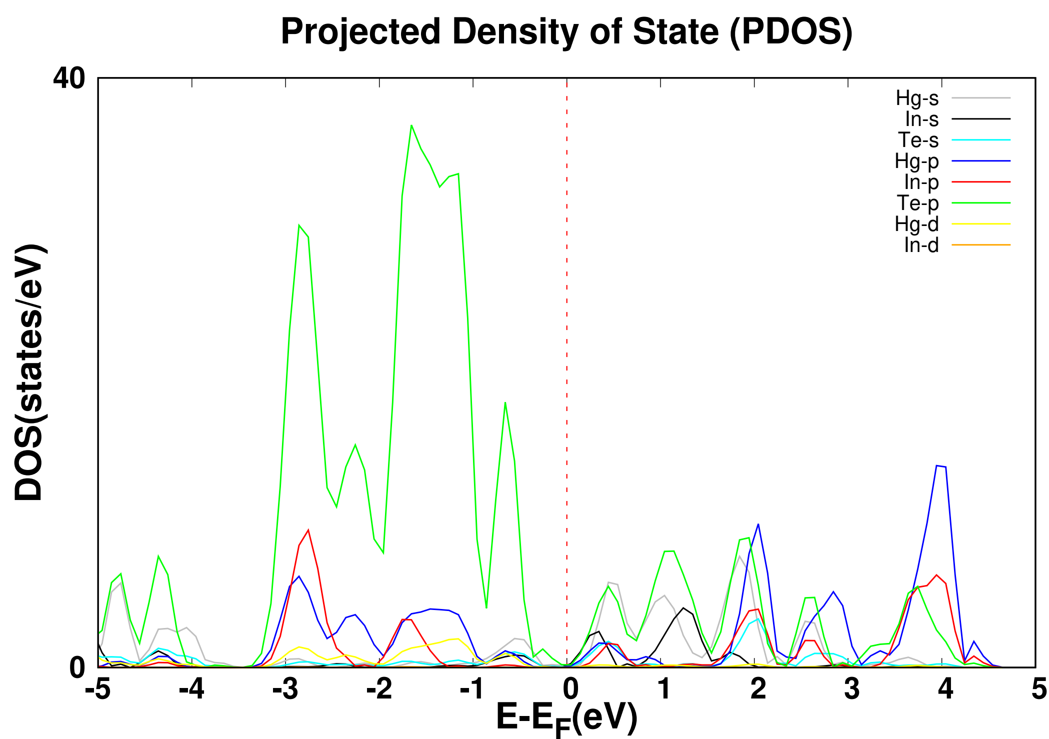

Figure 12: $Hg_5In_2Te_8$ projected density of state.

4.5 Effective mass of $Hg_5In_2Te_8$.

Effective mass calculations were performed using the finite difference method for Δk $(0.01, 0.005)$. These calculations were conducted for both the minimum conduction band and the maximum valence band.

4.5.1 Electron effective mass.

The tables 4 below display the electron effective mass values obtained with varying increments in k-point (Δk). It is evident that as Δk decreases, the reciprocal effective mass increases. Also, this can prove that the electron mobility increases as Δk decreases since the mobility is in inverse proportion to effective mass.

$\Delta k(2\pi/a)$	m_{xx}^{-1} (m_0)	m_{yy}^{-1} (m_0)	m_{zz}^{-1} (m_0)	m_{xy}^{-1} (m_0)	m_{xz}^{-1} (m_0)	m_{yz}^{-1} (m_0)
0.01	32.9407	32.9407	50.547	-2.839	-21.0139	-21.0139
0.005	34.0766	34.0766	54.5226	-6.815	-26.125	-26.125

Table 4: Electron effective mass at different Δk.

The effective mass tensor for $\Delta k = 0.005$ is:

$$\frac{1}{m_e^*} = \begin{bmatrix} 34.0766 & -6.815 & -26.125 \\ -6.815 & 34.0766 & -26.125 \\ -26.125 & -26.125 & 54.5226 \end{bmatrix} \tag{4.1}$$

To obtain effective mass in three directions we diagonalize the tensor matrix 4.1. The mathematical expression for the diagonalizing matrix is given by:

$$M = PDP^{-1} \tag{4.2}$$

Where D is diagonal matrix, P is Eigen vectors matrix and P^{-1} is inverse of P. The matrix 4.1 in diagonal form becomes:

$$\frac{1}{m_e^*} = \begin{bmatrix} -1 & 1.0145 & -0.4928 \\ 1 & 1.0145 & -0.4928 \\ 0 & 1 & 1 \end{bmatrix} \begin{bmatrix} 40.8916 & 0 & 0 \\ 0 & 1.5116 & 0 \\ 0 & 0 & 80.2725 \end{bmatrix} \begin{bmatrix} -0.5 & 0.5 & 0 \\ 0.3317 & 0.3317 & 0.3269 \\ -0.3317 & -0.3317 & 0.673 \end{bmatrix} \tag{4.3}$$

From this, the diagonal matrix is:

$$D = \begin{bmatrix} 40.8916 & 0 & 0 \\ 0 & 1.5116 & 0 \\ 0 & 0 & 80.2725 \end{bmatrix} \tag{4.4}$$

The electron's effective mass,

$$m_{ii}^* = \frac{1}{D_{ii}} \tag{4.5}$$

for $i = 1, 2, 3$. For the three components of diagonal matrix D, the effective mass is $m_{xx,e}^* = 0.024m_0$, $m_{yy,e}^* = 0.66m_0$, and $m_{zz,e}^* = 0.012m_0$ which are the diagonal elements of the diagonal matrix D. We can see that $m_{xx,e}^* = 0.024m_0$ and $m_{zz,e}^* = 0.012m_0$ is small compared to the Silicon, Germanium, and Gallium Arsenide electron effective mass as illustrated in Table 1.

4.5.2 Hole effective mass.

Table 5, the finite difference method used to calculate hole effective mass. It is calculated at difference Δk as shown in the table for all components. Compared to the electron effective mass, We can see that the hole effective mass is smaller than the electron effective mass. The negative sign in hole effective mass means that the force in $+$ direction will cause such an hole to move in $-$ direction. The small value of the hole's effective mass implies that the mobility is too high. The high mobility determines how the hole moves fast in the material.

$\Delta k(2\pi/a)$	m_{xx}^{-1} (m_0)	m_{yy}^{-1} (m_0)	m_{zz}^{-1} (m_0)	m_{xy}^{-1} (m_0)	m_{xz}^{-1} (m_0)	m_{yz}^{-1} (m_0)
0.01	-74.684	-74.684	-45.968	0.1419	1.4198	1.4198
0.005	-295.33	-295.33	-183.162	0.5679	5.3954	5.3954

Table 5: Hole effective mass at different Δk

The hole effective mass tensor for $\Delta k = 0.005$ is:

$$\frac{1}{m_h^*} = \begin{bmatrix} -295.33 & 0.5679 & 5.3954 \\ 0.5679 & -295.33 & 5.3954 \\ 5.3954 & 5.3954 & -183.162 \end{bmatrix} \tag{4.6}$$

We diagonalize the matrix 4.6 to obtain the diagonal elements. The mathematical expression for the diagonalizing matrix is given by:

$$M = PDP^{-1} \tag{4.7}$$

Where D is diagonal matrix, P is Eigen vectors matrix and P^{-1} is inverse of P. The matrix 4.6 in diagonal form becomes:

$$m_h^{*-1} = \begin{bmatrix} -1 & -10.39 & 0.048 \\ 1 & -10.39 & 0.048 \\ 0 & 1 & 1 \end{bmatrix} \begin{bmatrix} -295.8979 & 0 & 0 \\ 0 & -295.28 & 0 \\ 0 & 0 & -182.64 \end{bmatrix} \begin{bmatrix} -0.5 & 0.5 & 0 \\ -0.0479 & -0.0479 & 0.00461 \\ 0.0479 & 0.0479 & 0.995 \end{bmatrix} \tag{4.8}$$

From this, the diagonal matrix is:

$$D = \begin{bmatrix} -295.8979 & 0 & 0 \\ 0 & -295.28 & 0 \\ 0 & 0 & -182.64 \end{bmatrix} \tag{4.9}$$

The hole effective mass for three components is the diagonal elements of the matrix 4.9 ($m_{xx,h}^* = 0.0034m_0, m_{yy,h}^* = 0.0034m_0$ and $m_{zz,h}^* = 0.00547m_0$). We can see that all three components' effective masses are too small compared to the GaAs, Si, and Ge hole effective mass from Table 1.

4.6 Density of state effective mass.

The density of state effective mass m_{eDos}^* is a parameter that captures the curvature of the energy bands near the isotropic maxima or minima, enabling a simplified representation of the electronic structure. It is a key factor in understanding how electronic states are distributed in energy space and it is crucial for modeling charge carrier behaviors, especially in materials exhibiting parabolic band structures.
To obtain this parameter we considered the number of equivalent band minima M_c, longitudinal mass m_l, it is the mass which is the direction of the electric field, and two transverse masses m_t, the masses perpendicularly to the electric field.

$$m_{eDos}^* = Mc^{2/3}(m_l m_t m_t)^{1/3} \tag{4.10}$$

In this study, we assumed that the electric field applied in the x direction. So for $\Delta k = 0.005$ we obtain $m_l = 0.024m_0$, $m_t = 0.66m_0$ and $m_t = 0.012m_0$ and $M_c = 1$ for $Hg_5In_2Te_8$.
The value of density of state effective mass of $Hg_5In_2Te_8$ is $m_{eDos} = 0.057m_0$ This value is small compared to the density of state of Germanium $m_{eDos} = 0.56$, Silicon $m_{eDos} = 1.08$, and Gallium Arsenide $m_{eDos} = 0.67$ [37]. This means that $Hg_5In_2Te_8$ enhanced charge carrier mobility, implies that carriers with small effective mass respond more readily to applied electric fields, leading to high mobility and faster charge transport.

4.7 Effective mass for conductivity.

For more information, we also determine the effective mass for conductivity. It is the mass employed in conduction-related issues, taking into consideration the intricate structure of the semiconductor. these computations encompass the determination of mobility and diffusion constants. it is determined by:

$$m^*_{e,Cond} = \frac{3}{\frac{1}{m_l} + \frac{1}{m_t} + \frac{1}{m_t}} \tag{4.11}$$

So with $m_l = 0.024m_0$, $m_t = 0.66m_0$ and $m_t = 0.012m_0$, the effective mass for conductivity obtained is $m_{e,Cond} = 0.0238m_0$. This is small compared to the conductivity effective mass of Silicon ($m^*_{e,cond} = 0.26m_0$), Germanium ($m^*_{e,cond} = 0.12m_0$), and Gallium Arsenide ($m^*_{e,cond} = 0.067m_0$)[37].

4.8 Mobility

4.8.1 Electron mobility

Electron mobility measures how an electron can move through a material when an electric field is subjected to it. The higher mobility means that the electron can move faster in material. The value of relaxation timeτ used in this calculation is approximated to $2 \times 10^{-13}s$[38]. This task performed only for $\Delta k = 0.005$.

The mobility is given by:

$$\mu = \frac{e\tau}{m^*} \tag{4.12}$$

With $m^*_{xx,e} = 0.024m_0$, $m^*_{yy,e} = 0.66m_0$, and $m^*_{zz,e} = 0.012m_0$ and the value of relaxation time $\tau \approx 2 \times 10^{-13}$ the electron mobility in this three components are:

$$\mu_{e,xx} = 1.467m^2/(V.s) = 14670\,\text{cm}^2/(\text{V.s}) \tag{4.13}$$

$$\mu_{e,yy} = 0.0533m^2/(V.s) = 533\,\text{cm}^2/(\text{V.s}) \tag{4.14}$$

$$\mu_{e,zz} = 2.934m^2/(V.s) = 29340\,\text{cm}^2/(\text{V.s}) \tag{4.15}$$

The mobility is measured in $\text{m}^2/(\text{Vs})$. The effective electron mobility is the single value mobility which is obtained by combining these three components using Matthiessen's rule [39].

$$\frac{1}{\mu_{eff}} = \frac{1}{\mu_{xx}} + \frac{1}{\mu_{yy}} + \frac{1}{\mu_{zz}} \tag{4.16}$$

The effective mobility obtained is

$$\mu_{eff} = 0.05054m^2/(V.s) = 505.4\,\text{cm}^2/(\text{V.s}) \tag{4.17}$$

4.8.2 Hole mobility

Hole mobility measures how a hole can move through a material when an electric field is subjected to it. The higher hole mobility means that the hole can move faster in material. With $m^*_{xx,h} = 0.0034m_0, m^*_{yy,h} = 0.0034m_0$ and $m^*_{zz,h} = 0.00547m_0$ the hole mobility for these three components are:

$$\mu_{h,xx} = 10.3555m^2/(V.s) = 103555\,\text{cm}^2/(\text{V.s}) \tag{4.18}$$

$$\mu_{h,yy} = 10.3555m^2/(V.s) = 103555\,\text{cm}^2/(\text{V.s}) \tag{4.19}$$

$$\mu_{h,zz} = 6.4367m^2/(V.s) = 64367\,\text{cm}^2/(\text{V.s}) \tag{4.20}$$

this is higher than the hole mobility of Si, Ge, and GaAs as illustrated in Table1. This indicates that the hole can move very fast in the material when an electric field is applied to it. The effective hole mobility obtained is $\mu_{eff} = 2.8695m^2/(V.s) = 28695\,\text{cm}^2/(\text{V.s})$

5 Conclusion and Recommendation.

5.1 Conclusion

The findings of this study confirm that $Hg_5In_2Te_8$ exhibits significantly higher electron and hole mobilities compared to Silicon, Germanium, and Gallium Arsenide. The primary objective was to determine these mobilities and assess the material's potential applications based on its electrical conductivity properties. The electron mobility was found to be $14670\,\mathrm{cm^2/(V.s)}$, while the hole mobility was determined to be $103555\,\mathrm{cm^2/(V.s)}$, which is higher than the electron mobility. The electronic band structure analysis revealed an indirect band gap $E_g = 0.0567\,\mathrm{eV}$, and the computed density of states (DOS) supported the high carrier mobility. Furthermore, the effective masses of electrons and holes, calculated using the finite difference method, were $0.024m_0$ and $0.0034m_0$, explaining the high mobility of both carriers. These results indicate that $Hg_5In_2Te_8$ is an excellent material for various electronic applications, with significant potential for use in high-speed and high-efficiency electronic devices.

5.2 Recommendation

Based on our findings, it is evident that $Hg_5In_2Te_8$ is a high-mobility material. Because of the potential application of material with high mobility material, future studies should explore other properties of this material. Also, future studies can explore the effect of doping on the electron and hole mobility of this material.

References

[1] M Bordag. Drude model and lifshitz formula. *The European Physical Journal C*, 71:1–12, 2011.

[2] Wikipedia contributors. Drude model, 2024. Last modified January 15, 2024.

[3] Yanwei Liu, Yunlong Guo, and Yunqi Liu. High-mobility organic light-emitting semiconductors and its optoelectronic devices. *Small Structures*, 2(1):2000083, 2021.

[4] Jie Sun, Li Fu, Hongwei Liu, Yapeng Li, SP Ringer, and Zongwen Liu. On the morphology and crystallography of hg5in2te8 precipitation in hg3in2te6. *Journal of alloys and compounds*, 601:298–306, 2014.

[5] RC Smith. Device applications of the ternary semiconducting compounds. *Le Journal de Physique Colloques*, 36(C3):C3–89, 1975.

[6] Ana Claudia Arias, John D. MacKenzie, Iain McCulloch, Jonathan Rivnay, and Alberto Salleo. Materials and applications for large area electronics: Solution-based approaches. *Chemical Reviews*, 110(1):3–24, 2010.

[7] Stephen J Sweeney and Jayanta Mukherjee. Optoelectronic devices and materials. *Springer handbook of electronic and photonic materials*, pages 1–1, 2017.

[8] Yi Tian, Zhizhong Ge, An Sun, Zhipeng Zhu, Quan Zhang, Shuhui Lv, and Hongping Li. The impact of crystal structures on the magnetic and electronic properties in double perovskite sr2niteo6. *Chemical Physics Letters*, 754:137776, 2020.

[9] Zinaida M Grushka, Peter N Gorley, Olena G Grushka, Paul P Horley, Yarema I Radevych, and Zhuang Zhuo. Mercury indium telluride–a new promising material for photonic structures and devices. In *ICO20: Materials and Nanostructures*, volume 6029, pages 304–312. SPIE, 2006.

[10] SV Rakhmanova and EM Conwell. Electric-field dependence of mobility in conjugated polymer films. *Applied Physics Letters*, 76(25):3822–3824, 2000.

[11] Title of the webpage. URL, 2015. Accessed: Date.

[12] Mikhail I Katsnelson. Graphene: carbon in two dimensions. *Materials today*, 10(1-2):20–27, 2007.

[13] Nathan O Weiss, Hailong Zhou, Lei Liao, Yuan Liu, Shan Jiang, Yu Huang, and Xiangfeng Duan. Graphene: an emerging electronic material. *Advanced materials*, 24(43):5782–5825, 2012.

[14] SJ Zhang, SS Lin, XQ Li, XY Liu, HA Wu, WL Xu, P Wang, ZQ Wu, HK Zhong, and ZJ Xu. Opening the band gap of graphene through silicon doping for the improved performance of graphene/gaas heterojunction solar cells. *Nanoscale*, 8(1):226–232, 2016.

[15] Paolo Giannozzi, Stefano Baroni, Nicola Bonini, Matteo Calandra, Roberto Car, Carlo Cavazzoni, Davide Ceresoli, Guido L Chiarotti, Matteo Cococcioni, Ismaila Dabo, et al. Quantum espresso: a modular and open-source software project for quantum simulations of materials. *Journal of physics: Condensed matter*, 21(39):395502, 2009.

[16] Shiming Lei, Jingjing Lin, Yanyu Jia, Mason Gray, Andreas Topp, Gelareh Farahi, Sebastian Klemenz, Tong Gao, Fanny Rodolakis, Jessica L McChesney, et al. High mobility in a van der waals layered antiferromagnetic metal. *Science Advances*, 6(6):eaay6407, 2020.

[17] Shiming Lei, Jingj Lin, Yanyu Jia, Mason Gray, Andreas Topp, Gelareh Farahi, Sebastian Klemenz, Fanny Rodolakis, J. Mcchesney, Christian Ast, Ali Yazdani, Kenneth Burch, Sanfeng Wu, N. Ong, and Leslie Schoop. High mobility in a van der waals layered antiferromagnetic metal, 03 2019.

[18] SM Sze and JC Irvin. Resistivity, mobility and impurity levels in gaas, ge, and si at 300 k. *Solid-State Electronics*, 11(6):599–602, 1968.

[19] F. Schubert. Materials: Semiconductors silicon, germanium, and gaas, 2018. Accessed on 2023-10-31.

[20] Yiran Liang, Xuelei Liang, Zhiyong Zhang, Wei Li, Xiaoye Huo, and Lianmao Peng. High mobility flexible graphene field-effect transistors and ambipolar radio-frequency circuits. *Nanoscale*, 7(25):10954–10962, 2015.

[21] Lecture 17:anis.buet.ac.bd/teaching/properties$_of_materials$.

[22] The Materials Project. Materials data on in2hg5te8 by materials project.

[23] Hanak JJ. The? multiple-sample concept? in materials research: Synthesis, compositional analysis and testing of entire multicomponent systems. *Journal of Materials Science*, 5(11):964–971, 1970.

[24] Hidetsugu Nakayama, Shinji Sugahara, Mari Tokita, Kuniaki Fukuda, Masashi Mizumoto, Masato Abei, Junichi Shoda, Hideyuki Sakurai, Koji Tsuboi, and Koichi Tokuuye. Proton beam therapy for hepatocellular carcinoma: the university of tsukuba experience. *Cancer*, 115(23):5499–5506, 2009.

[25] Jie Sun, Li Fu, Hongwei Liu, SP Ringer, and Zongwen Liu. Interpretation of the vacancy-ordering controlled growth morphology of hg5in2te8 precipitates in hg3in2te6 single crystals by tem observation and crystallographic calculation. *Journal of Alloys and Compounds*, 622:206–212, 2015.

[26] Otfried Madelung. *Semiconductors: data handbook*. Springer Science & Business Media, 2004.

[27] H Tulsani. Differentiate between direct and indirect band gap semiconductors. *Retrieved October*, 9:2019, 2017.

[28] Laurent Lévy. Mercury telluride, a topological insulator with a helical spin texture. *New Trends in Topological Insulators, 3-6 June 2013*, 2013.

[29] Tetsuya Takimoto. Smb6: A promising candidate for a topological insulator. *Journal of the Physical Society of Japan*, 80(12):123710, 2011.

[30] M Zahid Hasan and Charles L Kane. Colloquium: topological insulators. *Reviews of modern physics*, 82(4):3045, 2010.

[31] Linghang Wang, Yangchun Dong, and Wanqi Jie. Growth, structure and electrical properties of mercury indium telluride single crystals. *Journal of Physics D: Applied Physics*, 40(13):3921, 2007.

[32] Robert E Newnham. *Properties of materials: anisotropy, symmetry, structure*. Oxford university press, 2005.

[33] GA Saunders and T Seddon. Effect of ordered vacancies on ultrasonic wave propagation in some mercury-indium tellurides. *Journal of Physics and Chemistry of Solids*, 31(11):2495–2504, 1970.

[34] T Alper, NG Pace, and GA Saunders. The elastic constants of hg5in2te8. *Journal of Physics D: Applied Physics*, 1(8):1079, 1968.

[35] HA Rahnamaye Aliabad, Hadi Arabshahi, and A Hamel Aliabadi. The effect of hubbard potential on effective mass of carriers in doped indium oxide. *Int. J. Phys. Sci*, 7:696–708, 2012.

[36] Anthony P Nicholson. *Density functional theory and Green's function approach to investigate cadmium telluride based thin film photovoltaics*. PhD thesis, Colorado State University, 2020.

[37] S Dimitrijev. Effective mass in semiconductors. bart j. van zeghbroeck; 1997.

[38] VT Dolgopolov, AA Shashkin, SI Dorozhkin, and EA Vyrodov. Energy relaxation time in a two-dimensional electron gas at a (001) surface of silicon. *Zh. Eksp. Teor. Fiz*, 89:2113–2123, 1985.

[39] Ming-Jer Chen, Wei-Han Lee, and Yi-Hui Huang. Error-free matthiessen's rule in the mosfet universal mobility region. *IEEE transactions on electron devices*, 60(2):753–758, 2013.